Slow-light interferometry: practical limitations to spectroscopic performance

Zhimin Shi* and Robert W. Boyd

The Institute of Optics, University of Rochester, Rochester, New York 14627 USA
**Corresponding author: zshi@optics.rochester.edu*

Received April 17, 2008; accepted September 4, 2008;
posted September 17, 2008 (Doc. ID 94991); published October 24, 2008

We investigate how the use of slow-light methods can enhance the performance of various types of spectroscopic interferometers under practical conditions. We show that, while in ideal cases the enhancement of the spectral resolution is equal to the magnitude of the group index of the slow-light medium, the ratio between the associated gain or loss and the group index of the slow-light medium actually determines the spectral resolution under more-general conditions. Moreover, the dispersion of this ratio leads to frequency-dependent spectral resolution, which limits the useful working bandwidth of the interferometer. We also evaluate the performance of interferometers using three specific slow-light processes in terms of the achievable spectral resolution and the effective working finesse. We show that the spectral resolution is typically limited by the characteristic linewidth of each slow-light process and that there is no fundamental upper limit for the effective working finesse.

OCIS codes: 120.3180, 120.6200, 120.5050, 260.2030.

1. INTRODUCTION

Slow- and fast-light technology [1] has recently attracted a great deal of interest, both in terms of fundamental [2–5] and practical [6–11] aspects. One of the promising potential applications of slow light is in optical communications, where a tunable delay element can be used for all-optical buffering, data-synchronization, jitter correction, etc. One primary figure of merit of a slow-light delay element is the maximum fractional delay (also known as the delay-bandwidth product). While there is no fundamental limit for this figure of merit [12], it is often limited by the maximum change in signal power level and the signal distortion that a practical system can tolerate [13].

It has been shown recently that slow light can also be used to enhance the spectral performance of various types of interferometers [14–17]. The ability to increase the spectral resolution of interferometric spectrometers by a factor as large as the group index can have many important implications for modern optical technology. Increased resolution leads to the ability to resolve closely spaced spectral components. This ability can prove extremely important for applications in analytic chemistry and biology. Alternatively, spectrometers could be made very much smaller (by a factor as large as the group index) without suffering any degradation of their spectral resolution. Such miniaturized spectrometers could have important implications in the context of integrated optical systems. Applications of such chip-scale spectrometers could include the design of improved wavelength-division multiplexers, extremely narrow tunable filters, and general-purpose spectrometers and the measurement of small frequency shifts.

In the ideal case in which the slow-light medium is lossless and has uniform group index over the bandwidth of interest, the enhancement factor of the spectral resolution is equal to the group index of the slow-light medium. However, in practice, a slow-light medium typically has associated gain or loss and has dispersion of the group index, which limit the maximum achievable enhancement of the spectral performances. In this paper, we investigate the spectral performance of various types of slow-light interferometers, and we investigate in detail how the gain or loss and dispersion of the group index influence the spectral performance.

We use two figures of merit to evaluate the spectral performance of an interferometer. The first one is the spectral resolution $\delta\nu_{\min}$, which describes the minimum frequency difference that the interferometer can resolve. This quantity also describes how sensitive an interferometer is to the change of the input frequency when it is used as a frequency monitor or sensor.

Second, the maximum usable spectral bandwidth of an interferometer, which we call the working bandwidth, is an important quantity. The working bandwidth can be limited by both the dispersive properties of the slow-light medium and by the construction of the interferometer itself. In this paper, we consider only the limitation imposed by the dispersive properties of the medium, which would usually be the primary limitation for a practical slow-light interferometer. We determine the working bandwidth of the interferometer by setting a uniformity criterion such that the spectral resolution within the working bandwidth should not vary by more than a certain fractional amount. To describe this property ad-

equately, we use a second figure of merit, namely, the working finesse $\mathcal{F}_w$, which is defined as the ratio of the working bandwidth to the spectral resolution.

2. SPECTRAL PERFORMANCE OF SLOW-LIGHT INTERFEROMETERS

In this section, we derive expressions for the frequency-dependent spectral resolution $\delta\nu_{\min}$ of three types of commonly used spectroscopic interferometers, namely, the two-beam interferometer, the multiple-beam interferometer, and the Fourier transform (FT) interferometer, for cases in which slow-light media are used. Note that the working finesse is not treated in this section because this concept can be treated only within the context of specific model of the slow-light medium, which are discussed in Section 3.

A. Two-Beam Interferometer

First, we consider the case of a Mach–Zehnder (M–Z) interferometer as a typical example of a two-beam interferometer. A slow-light medium of length L is placed in one of its arms (see Fig. 1) and the two arms are adjusted so that the optical path difference between the arms is equal to the optical path length through the slow-light medium. The transmission of such an interferometer is then given by

$$T = \frac{1}{4}(1 + e^{-\alpha L} + 2e^{-0.5\alpha L}\cos\Delta\phi), \tag{1}$$

where α is the absorption coefficient of the medium, and $\Delta\phi$ is the phase difference between the two arms expressed by

$$\Delta\phi(\nu) = \frac{2\pi\nu}{c}n(\nu)L, \tag{2}$$

and where ν is the frequency of the input field, c is the speed of light in vacuum, and $n(\nu)$ is the refractive index of the slow-light medium.

The spectral sensitivity of such an interferometer can be described by the rate at which the phase difference term $\Delta\phi$ changes with frequency ν. Taking the derivative of $\Delta\phi$ with respect to frequency, one obtains the following expression:

$$\frac{d\Delta\phi}{d\nu} = \frac{d}{d\nu}\left(\frac{2\pi\nu n(\nu)L}{c}\right) = \frac{2\pi L}{c}\left(n + \nu\frac{dn}{d\nu}\right) = \frac{2\pi L n_g}{c}, \tag{3}$$

where $n_g \equiv n + \nu dn/d\nu$ is the group index. If one defines the spectral resolution $\delta\nu_{\min}$ to be the frequency difference between adjacent transmission peaks and valleys, one obtains the following expression for the spectral resolution:

$$\delta\nu_{\min} = \frac{c}{2Ln_g}. \tag{4}$$

Note also that the visibility of such a M–Z interferometer is given by

$$\mathcal{V} \equiv \frac{I_{\text{out,max}} - I_{\text{out,min}}}{I_{\text{out,max}} + I_{\text{out,min}}} = \frac{2e^{-0.5\alpha L}}{1 + e^{-\alpha L}}. \tag{5}$$

For a lossless M–Z interferometer, the value of the visibility $\mathcal{V}$ is 1. The associated loss or gain of the slow-light medium will decrease the fringe visibility $\mathcal{V}$. For definiteness, we require that the loss through the slow-light medium be less than $1/e$ (or gain less than a factor of e), and consequently we obtain the following restriction on the length L of the medium:

$$|\alpha L| \leq 1. \tag{6}$$

Note that this requirement indicates that the visibility $\mathcal{V}$ is always no less than 0.65. Substituting this requirement into Eq. (4), one obtains the following expression for the minimum spectral resolution for a M–Z interferometer with a lossy slow-light medium:

$$\delta\nu_{\min} = \left|\frac{c\alpha}{2n_g}\right|. \tag{7}$$

Such an expression for the spectral resolution is also applicable to other types of two-beam interferometers, such as a Michelson interferometer.

B. Multiple-Beam Interferometer

To investigate the performance of multiple-beam interferometers, we use as a typical example the Fabry–Perot (F–P) interferometer (see Fig. 2). For the case in which the F–P etalon is a slow-light medium of thickness L, the transmission of the interferometer as a function of the incidence angle θ within the medium is given by [18],

$$T(\theta) \approx \frac{T_s^2 T_L(\theta)}{(1 - R_s T_L(\theta))^2}\frac{1}{1 + \mathcal{F}^2\sin^2\Delta\phi(\theta)}, \tag{8}$$

where T_s and R_s are the transmissivity and reflectivity at the air–medium interface (as well as the medium–air interface), respectively, $T_L(\theta) \equiv \exp(-\alpha L/\cos\theta)$ is the transmissivity of a plane wave at incident angle θ through the medium, $\Delta\phi = kL\cos\theta + \psi_0$ is the phase difference term, α and k are the absorption coefficient and the wave number of the field inside the slow-light medium,

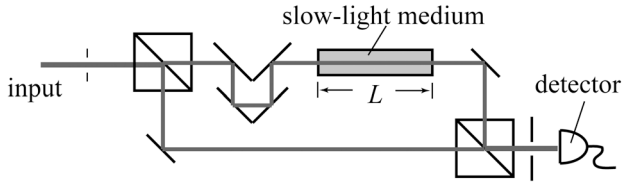

Fig. 1. (Color online) Schematic diagram of a M–Z interferometer containing a slow-light medium in one arm.

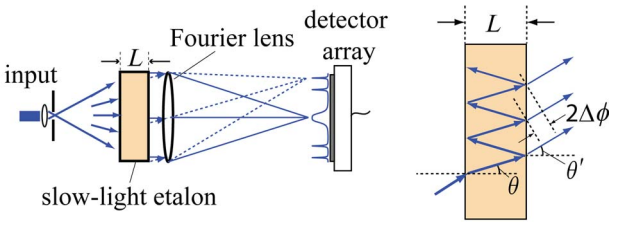

Fig. 2. (Color online) Schematic diagram of a slow-light F–P interferometer (left). A close look at the multiple beam interference within the F-P etalon (right).

respectively, ψ_0 is the phase change of field due to reflection at the medium–air interface, and $\mathcal{F}$ is the finesse defined as $\mathcal{F}\equiv 2R_s^{0.5}T_L(\theta)/[1-R_sT_L(\theta)]$.

The angle between the center of the mth fringe and the normal direction is given by

$$\theta_m = \cos^{-1}\left(1-\frac{(M-m)\lambda}{2Ln}\right), \tag{9}$$

where $M\approx 2Ln/\lambda$ is the order of the fringe at normal incidence. The spectral sensitivity of the mth order fringe is therefore given by

$$\frac{d\theta_m}{d\lambda} = \frac{M-m}{2L\sin\theta_m}\left(\frac{1}{n}-\frac{\lambda dn}{n^2 d\lambda}\right) = \frac{(M-m)n_g}{2n^2L\sin\theta_m}. \tag{10}$$

For the case in which the finesse is high (i.e., small angular spread of the fringes), the angular spread [full width at half maximum (FWHM)] of the mth order fringe is determined through the relation $\delta\Delta\phi_m=2/\mathcal{F}$ and is given by

$$\delta\theta_m = \frac{\lambda}{\pi Ln\sin\theta_m\mathcal{F}}. \tag{11}$$

Thus, the spectral resolution of the mth order fringe is given by

$$\delta\lambda_m = \frac{d\lambda}{d\theta}\delta\theta_m = \frac{2n\lambda}{(M-m)n_g\pi\mathcal{F}}. \tag{12}$$

For a F–P interferometer, one typically has the relation $M\gg m$. Thus, one can obtain the following expression for the spectral resolution of a F–P interferometer:

$$\delta\lambda_{\min}\approx\frac{2n\lambda}{Mn_g\pi\mathcal{F}} = \frac{\lambda^2}{n_gL\pi\mathcal{F}}. \tag{13}$$

To see more clearly how the absorption or gain of the slow-light medium influence the spectral resolution, we can introduce the definition of $\mathcal{F}$ into the above expression. When the fractional loss or gain of the field after a single pass through the slow-light medium is small, the above expression can be approximated by

$$\delta\lambda_{\min}\approx\frac{\lambda^2(1+\alpha L-R_s)}{2n_gL\pi} = \left|\frac{\lambda^2(1-R_s)}{2n_gL\pi}+\frac{\lambda^2\alpha}{2n_g\pi}\right|, \tag{14}$$

or in frequency units

$$\delta\nu_{\min} = \left|\frac{c(1-R_s)}{2\pi n_gL}+\frac{c\alpha}{2\pi n_g}\right|. \tag{15}$$

One sees that the resolution is given by the sum of two terms. The first term is present even for a lossless interferometer and is inversely proportional to the group index n_g. The second term is proportional to the ratio between α and n_g. In principle, the first term can be made to vanish when the reflectivity at the surface R_s approaches unity. In such cases, the overall spectral resolution will be determined primarily by the second term such that

$$\delta\nu_{\min}\approx\left|\frac{c\alpha}{2\pi n_g}\right|. \tag{16}$$

Note that if the slow-light medium has gain such that the single-pass gain gL is comparable to the loss at the reflection $1-R_s$, the two terms in Eq. (15) would become comparable to each other but with opposite signs. In this case, one can obtain very-high spectral resolution as long as the gain is not saturated. Note that the expression of Eq. (15) is also valid for other types of multiple-beam interferometer, such as a wedged shear interferometer [15].

C. Fourier Transform Interferometer

Recently, it has been proposed and experimentally demonstrated that one can construct a FT interferometer using the method of variable slow light [17]. As shown in Fig. 3, such a FT interferometer typically contains two fixed arms, with a variable slow-light medium in one arm. The two arms are adjusted to have zero optical-path-length difference when the reduced group index $n_g'=n_g-n$ of the variable slow-light medium is zero. In the ideal case in which the slow-light medium is lossless and has a uniform group index over the bandwidth of interest, the output I_{out} (see Fig. 3) of such a slow-light FT interferometer is given by [17]

$$I_{\text{out}}(\tau_g) = \Re\left\{\int_{-\infty}^{\infty} I_{\text{in}}(\nu_0+\nu')e^{i2\pi\nu'\tau_g}d\nu'\right\}, \tag{17}$$

where ν_0 is a reference frequency at which $n(\nu_0)$ is independent of the reduced group index n_g' (cf. Ref. [17]) and $\tau_g=n_g'L/c$ is the group delay between the two arms of the interferometer, which can be varied from zero to a maximum value $\tau_{g,\max}$.

Similar to a conventional FT interferometer, the spectral resolution of such an ideal slow-light FT interferometer is limited by the maximum group delay between the two arms through the following relation:

$$\delta\nu_1 = \frac{1}{2\tau_{g,\max}} = \frac{c}{2n_{g,\max}'L}. \tag{18}$$

In practice, however, a variable slow-light medium typically has associated frequency-dependent loss, which is usually linearly proportional to the reduced group index n_g'. In this case, the output of the interferometer can be rewritten in the following form:

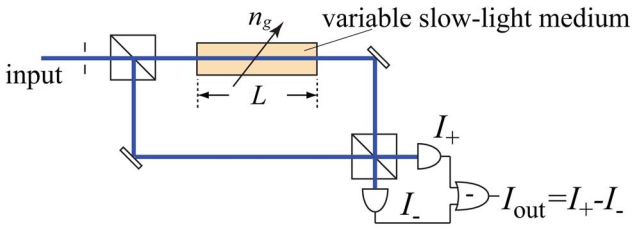

Fig. 3. (Color online) Schematic diagram of a slow-light FT interferometer. The reduced group index of the variable slow-light medium can be increased from zero to a maximum value.

$$I_{\text{out}}(\tau_g) = \Re\left\{\int_{-\infty}^{\infty} I_{\text{in}}(\nu_0+\nu')e^{-\alpha(\nu_0+\nu')/2L}e^{i2\pi\nu'\tau_g}\mathrm{d}\nu'\right\}. \tag{19}$$

For an input field containing only an infinitely narrow spectral line centered at ν_1, the output as a function of the group delay is given by

$$I'_{\text{out}} = \Re\{e^{-0.5\alpha(\nu_1)L}e^{i2\pi(\nu_1-\nu_0)\tau_g}\}. \tag{20}$$

To retrieve the input spectrum, one needs to take the FT of the output $I_{\text{out}}(\tau'_g)$ as follows:

$$\begin{aligned} I_{\text{in}} &= \text{FT}\{\Re\{e^{-0.5\alpha(\nu_1)L}e^{i2\pi(\nu_1-\nu_0)\tau_g}\}\} \\ &= \int_{-\infty}^{\infty} e^{-\alpha(\nu_1)L/2\tau_g|\tau_g|}e^{-i2\pi\tau_g(\nu'-\nu_1+\nu_0)}\mathrm{d}\tau_g \\ &= \int_{-\infty}^{\infty} e^{-\sigma|\tau_g|}e^{-i2\pi\tau_g\nu''}\mathrm{d}\tau_g, \end{aligned} \tag{21}$$

where $\sigma \equiv \alpha(\nu')L/(2\tau_g)$ and $\nu'' \equiv \nu' - \nu_1 + \nu_0$ is the frequency detuning from ν'. Note that σ is independent of τ_g. Consequently, one can calculate the above FT as follows:

$$\begin{aligned} I_{\text{in}}(\nu'') &= \int_0^{\infty} e^{-\sigma\tau_g}e^{-i2\pi\tau_g\nu''}\mathrm{d}\tau_g + \int_{-\infty}^{0} e^{\sigma\tau_g}e^{-i2\pi\tau_g\nu''}\mathrm{d}\tau_g \\ &= \frac{1}{\sigma+i2\pi\nu''} + \frac{1}{\sigma-i2\pi\nu''} = \frac{C}{\nu''^2+\gamma_{\text{eff}}^2}, \end{aligned} \tag{22}$$

where C is a constant independent of ν'' and γ_{eff} is the effective linewidth given by

$$\gamma_{\text{eff}} = \frac{\sigma}{2\pi} = \frac{c\alpha}{4\pi n'_g}. \tag{23}$$

One sees that the retrieved spectrum is a Lorentzian-shaped line with a FWHM linewidth of $\delta\nu_2 = 2\gamma_{\text{eff}} = c\alpha/2\pi n'_g$. Thus, the overall spectral resolution of the slow-light FT interferometer is given by

$$\delta\nu_{\min} = \max\left[\frac{c}{2n'_{g,\max}L}, \frac{c\alpha}{2\pi n'_g}\right]. \tag{24}$$

Since L can be arbitrarily large, the spectral resolution will be primarily limited by the second contribution.

3. INTERFEROMETER PERFORMANCE FOR SPECIFIC SLOW-LIGHT TECHNIQUES

There are many physical processes that have been proposed and demonstrated to realize slow and fast light. Here we investigate the performance of slow-light interferometers using three specific slow-light mechanisms. As shown in Section 2, the spectral resolutions of the three types of interferometers we consider in this paper are limited by $|c\alpha/(2n_g)|$, $|c\alpha/(2\pi n_g)|$, and $|c\alpha/(2\pi n'_g)|$, respectively. We define the characteristic spectral resolution as $\delta\nu_c \equiv |c\alpha/(2\pi n'_g)|$ for the remainder the paper. Note also that we assume that the group index n_g is much larger than the refractive index n such that $n'_g \approx n_g$.

The working bandwidth $\Delta\nu_w$ of a slow-light medium is calculated such that the characteristic spectral resolution within the working bandwidth does not vary by more than a factor of 2. The working finesse $\mathcal{F}_w = \Delta\nu_w/\delta\nu_c$ is calculated accordingly.

A. Single Isolated Gain Line

Single-resonance gain features are commonly used to achieve slow light [6,19–21] because of the rapid change of the refractive index in the vicinity of the resonance center. For example, the gain coefficient, refractive index, and reduced group index of an unsaturated Lorentzian gain line [6,19] as functions of the frequency detuning $\nu' = \nu - \nu_0$ from the resonance center ν_0 are given by

$$g(\nu') = g_0\frac{\gamma^2}{\nu'^2+\gamma^2}, \tag{25}$$

$$n(\nu') = n(0) + \frac{g_0}{2k_0}\frac{\gamma\nu'}{\nu'^2+\gamma^2}, \tag{26}$$

and

$$n'_g(\nu') = \frac{cg_0\gamma}{4\pi}\frac{-\nu'^2+\gamma^2}{(\nu'^2+\gamma^2)^2}, \tag{27}$$

where g_0 and k_0 are the gain coefficient and the wave number at the center frequency ν_0, respectively, γ is the half width at half maximum (HWHM) linewidth, and $n(0)$ is the background refractive index at the resonance center.

From the above expressions, one can obtain the ratio between g and n'_g as

$$\frac{g(\nu')}{n'_g(\nu')} = -\frac{4\pi\gamma}{c}\frac{\nu'^2+\gamma^2}{\nu'^2-\gamma^2}. \tag{28}$$

The characteristic spectral resolution at the resonance center is then given by

$$\delta\nu_c(\nu'=0) = \left|\frac{c\alpha(0)}{2\pi n'_g(0)}\right| = 2\gamma. \tag{29}$$

One sees from Eq. (28) that the spectral resolution is frequency dependent and deteriorates as the frequency moves away from the resonance center. The working bandwidth is determined through the relation $\delta\nu_c(\nu' = 0.5\Delta\nu_w) = 2\delta\nu_c(\nu'=0)$ and is given by

$$\Delta\nu_w = \frac{2\gamma}{\sqrt{3}}. \tag{30}$$

Consequently, the working finesse $\mathcal{F}_w$ is given by

$$\mathcal{F}_w = \frac{1}{\sqrt{3}}. \tag{31}$$

We see that the working finesse is independent of the linewidth of the resonance, and is less than unity, which is due to the rapid change in spectral resolution [see Fig. 4(b)] caused by the rapid variation of the group index and

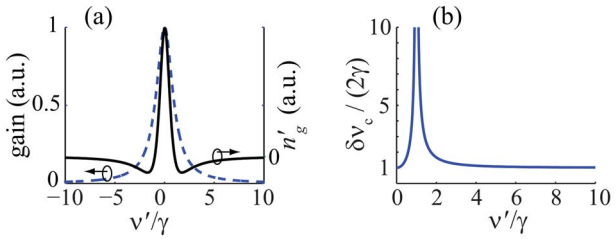

Fig. 4. (Color online) (a) The reduced group index n_g' and gain coefficient g and (b) the characteristic spectral resolution $\delta\nu_c$ as functions of the normalized frequency detuning from the resonance center for a single-Lorentzian-gain-line medium.

the gain coefficient in the vicinity of a Lorentzian resonance center [see Fig. 4(a)]. This result indicates that such a slow-light medium may be useful for detecting the frequency shift of an input field, but is not suitable for constructing a spectrometer to measure a broad spectrum because of its very limited working finesse near the resonance center.

Two techniques can be used to overcome this limitation. One is to use a broadened gain feature with a flattened top (e.g., using multiple gain lines [20,21]) instead of a single Lorentzian gain line to increase the working bandwidth. The other is to put the gain feature on a broadband absorption background to make the medium transparent near the resonance center. Using the latter technique, one can make the absolute magnitude of the gain coefficient be very small near the resonance center and, consequently, achieve high spectral resolution because the characteristic spectral resolution will no longer be restricted by Eq. (29).

Note, however, that the ratio given by Eq. (28) does not change much in the wings of the resonance when the frequency detuning ν' is much larger than γ [also see Fig. 4(b)]. This result indicates that such a slow-light medium can be used in a spectrometer if the working frequency range is chosen to be in the wing of the resonance center [17] so long as the strength of the resonance is great enough to provide a large group index in the wing region.

B. Separated Double Absorption Lines

It has recently been shown that the use of the transparency window between two separated absorption features is a very effective technique to realize slow light [10,11]. Here we consider the case in which two identical Lorentzian resonance lines of HWHM linewidth γ, separated by 2Δ, are used. The absorption coefficient, relative refractive index $n'(\nu')\equiv n(\nu')-n(\nu'=0)$, and reduced group index as functions of the detuning $\nu'=\nu-\nu_0$ from the center frequency ν_0 halfway between the two resonance lines are given by

$$\alpha(\nu')=\alpha_0\left[\frac{\gamma^2}{(\nu'-\Delta)^2+\gamma^2}+\frac{\gamma^2}{(\nu'+\Delta)^2+\gamma^2}\right], \tag{32}$$

$$n'(\nu')=-\frac{\alpha_0}{2k_0}\left\{\frac{\gamma(\nu'-\Delta)}{(\nu'-\Delta)^2+\gamma^2}+\frac{\gamma(\nu'+\Delta)}{(\nu'+\Delta)^2+\gamma^2}\right\}, \tag{33}$$

and

$$n_g'=\frac{c\alpha_0\gamma}{4\pi}\left[\frac{(\nu'-\Delta)^2-\gamma^2}{[(\nu'-\Delta)^2+\gamma^2]^2}+\frac{(\nu'+\Delta)^2-\gamma^2}{[(\nu'+\Delta)^2+\gamma^2]^2}\right]. \tag{34}$$

Thus, the ratio between n_g' and α is given by

$$\frac{n_g'(\nu')}{\alpha(\nu')}=\frac{c}{4\pi}\left[\frac{1}{\gamma}+\frac{2\gamma}{\nu'^2+\gamma^2+\Delta^2}-\frac{2\gamma}{(\nu'-\Delta)^2+\gamma^2}-\frac{2\gamma}{(\nu'+\Delta)^2+\gamma^2}\right]. \tag{35}$$

The characteristic spectral resolution at the center frequency ν_0 is thus given by

$$\delta\nu_c(\nu'=0)=\left|\frac{c\alpha(0)}{2\pi n_g'(0)}\right|=2\gamma\frac{\Delta^2+\gamma^2}{\Delta^2-\gamma^2}. \tag{36}$$

For the case in which the half separation Δ between the two resonance centers is much larger than the resonance linewidth γ, $\delta\nu_c$ is approximately equal to 2γ [see Fig. 5(b)].

Note that in the cases in which $\Delta\gg\gamma$, the working bandwidth is approximately equal to the separation between the two resonances 2Δ. Therefore, the working finesse in this case can be approximated by

$$\mathcal{F}_w\approx\frac{\Delta}{\gamma}. \tag{37}$$

As long as the strength of the resonances is great enough, the working finesse can be very high and linearly proportional to the separation between the two resonance centers [see Fig. 5(c)]. Note that we require that the reduced group index within the entire working bandwidth be of the same sign (either positive or negative for slow-or fast-light cases, respectively). Thus, the working finesse becomes zero when $\Delta=\gamma$. For $\Delta<\gamma$ the double-resonance medium becomes a single-absorption-line medium, and therefore the working finesse is also reduced to that of a single-gain-line medium.

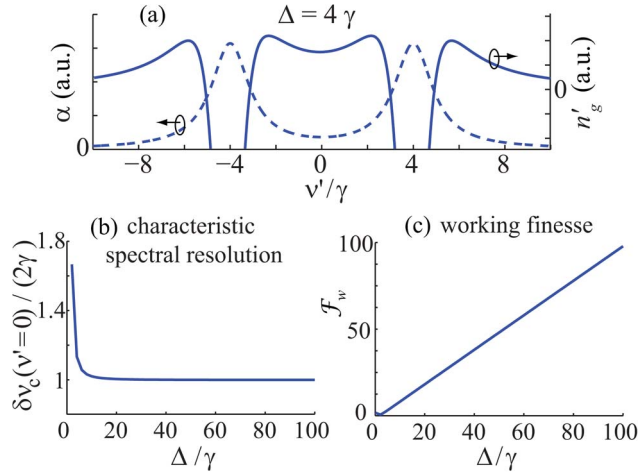

Fig. 5. (Color online) (a) The reduced group index and absorption coefficient as functions of detuning for a double-absorption-line medium with $\Delta=4\gamma$. (b) The characteristic spectral resolution at $\nu'=0$. and (c) The working finesse as functions of the normalized half separation between the two resonance centers.

C. Electromagnetically Induced Transparency

Electromagnetically induced transparency (EIT) is another slow-light process that can achieve a very large group index [2,22,23]. In the case of zero pump detuning [see Fig. 6(a)], the analytic expression for the complex refractive index of a Λ-type EIT medium as a function of the frequency detuning $\nu' = \nu - \nu_0$ from the EIT resonance center ν_0 is given by [1]

$$\tilde{n}(\nu') = \frac{\alpha_0}{2k_0}\frac{\gamma_{ba}(\nu' + i\gamma_{ca})}{|\Omega_p|^2 - (\nu' + i\gamma_{ba})(\nu' + i\gamma_{ca})}, \tag{38}$$

where α_0 and k_0 are the background absorption coefficient (when the pump field is absent) and the wave number at the EIT center frequency, respectively; γ_{ca} and γ_{ba} are the dephasing rates of the transitions from levels $|c\rangle$ to $|a\rangle$ and from $|b\rangle$ to $|a\rangle$, respectively; and Ω_p is the pump Rabi frequency.

For a typical EIT medium with $\gamma_{ba} \gg \gamma_{ca}$, one can expand Eq. (38) in a Taylor series, keep terms up to the third order, and obtain the following approximate expressions for the absorption coefficient and the refractive index near the EIT resonance center (within the transparency window),

$$\alpha(\nu') \approx \frac{\alpha_0}{1 + |\bar{\Omega}_p|^2}\left(1 + \frac{\nu'^2}{A^2}\right), \tag{39}$$

and

$$n(\nu') \approx 1 + \frac{\alpha_0 c}{4\pi\nu_0}\frac{B\nu'}{1 + |\bar{\Omega}_p|^2}\left(1 + \frac{\nu'^2}{C^2}\right), \tag{40}$$

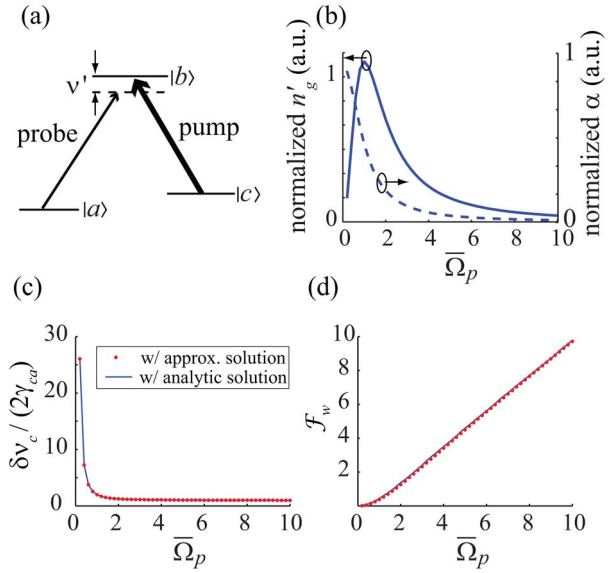

Fig. 6. (Color online) (a) Energy-level diagram of a Λ-type EIT system. (b) The reduced group index and absorption coefficient at the center frequency. (c) The characteristic spectral resolution at $\nu' = 0$. (d) The working finesse plotted as functions of the normalized pump Rabi frequency for an EIT medium with $\bar{\gamma} = 100$. The dots are results using the approximate expression of Eqs. (43) and (46), and the solid lines are results based on the analytical expression of Eq. (38).

where $\bar{\Omega}_p \equiv \Omega_p/\sqrt{\gamma_{ba}\gamma_{ca}}$ is the normalized pump Rabi frequency, $\bar{\gamma} \equiv \gamma_{ba}/\gamma_{ca}$, $A^2 \equiv \gamma_{ba}^2(1 + |\bar{\Omega}_p|^2)^2/[(\bar{\gamma}^2 + 2\bar{\gamma})|\bar{\Omega}_p|^2 - 1]$, $B \equiv (|\bar{\Omega}_p|^2 - \bar{\gamma}^{-1})/[\gamma_{ca}(1 + |\bar{\Omega}_p|^2)]$, and $C^2 \equiv \gamma_{ca}\gamma_{ba}(|\bar{\Omega}_p|^2 + 1)^2(|\bar{\Omega}_p|^2 - \bar{\gamma}^{-1})/[|\bar{\Omega}_p|^4 - (3\bar{\gamma}^{-1} + \bar{\gamma} + 2)|\bar{\Omega}_p|^2 + \bar{\gamma}^{-2}]$.

The reduced group index n_g' is then given by

$$n_g'(\nu') = \frac{\alpha_0 c}{4\pi}\frac{B}{|\bar{\Omega}_p|^2 + 1}\left(1 + \frac{3\nu'^2}{C^2}\right). \tag{41}$$

Using these expressions, one can obtain the following result for the ratio of α to n_g':

$$\frac{\alpha(\nu')}{n_g'(\nu')} = \frac{4\pi C^2}{cBA^2}\frac{(A^2 + \nu'^2)}{(C^2 + 3\nu'^2)}. \tag{42}$$

At the EIT resonance center (i.e., $\nu' = 0$), one obtains the following expression for the characteristic spectral resolution:

$$\delta\nu_c(\nu' = 0) = \left|\frac{c\alpha(0)}{2\pi n_g'(0)}\right| = \frac{2}{B} = 2\gamma_{ca}\frac{|\bar{\Omega}_p|^2 + 1}{|\bar{\Omega}_p|^2 - \bar{\gamma}^{-1}}. \tag{43}$$

As the pump Rabi frequency increases, the characteristic spectral resolution approaches its minimum value $\delta\nu_c \to 2\gamma_{ca}$. Note that this resolution is much finer than the intrinsic linewidth γ_{ba} associated with the transition from level $|b\rangle$ to $|a\rangle$.

One sees from Eq. (42) that the resolution $\delta\nu_c$ will deteriorate as the signal frequency is detuned away from the EIT resonance center. The working bandwidth $\Delta\nu_w$ is determined through the relation that the resolution at the boundary $\delta\nu_c(\nu' = 0.5\Delta\nu_w)$ of the working bandwidth is twice as large as the resolution at the EIT resonance center, i.e.,

$$\frac{A^2 + (0.5\Delta\nu_w)^2}{C^2 + 3(0.5\Delta\nu_w)^2} = 2\frac{A^2}{C^2}. \tag{44}$$

For a large pump Rabi frequency, one obtains the following expression for the working bandwidth:

$$\Delta\nu_w = 2\sqrt{\frac{A^2C^2}{C^2 - 6A^2}} \approx \frac{2\gamma_{ba}|\bar{\Omega}_p|}{\sqrt{\bar{\gamma}(\bar{\gamma} - 5)}}. \tag{45}$$

Since $\gamma_{ba} \gg \gamma_{ca}$ (i.e., $\bar{\gamma} \gg 1$), the working bandwidth can be further approximated as $\Delta\nu_w \approx 2\gamma_{ca}|\bar{\Omega}_p|$. Consequently, the working finesse $\mathcal{F}_w$ is given by

$$\mathcal{F}_w = B\sqrt{\frac{A^2C^2}{C^2 - 6A^2}} = \frac{|\bar{\Omega}_p|^2 + 1}{|\bar{\Omega}_p|^2 - \bar{\gamma}^{-1}}\sqrt{\frac{\bar{\gamma}}{\bar{\gamma} - 5}}|\bar{\Omega}_p|. \tag{46}$$

For a large pump Rabi frequency and a large $\bar{\gamma}$, the working finesse becomes $\mathcal{F}_w \approx |\bar{\Omega}_p|$, i.e., the normalized pump Rabi frequency.

Figure 6(b) shows the normalized reduced group index and the absorption coefficient at the EIT resonance center

as the normalized pump Rabi frequency $\bar{\Omega}_p$ increases. One sees that the group index reaches its maximum when $\bar{\Omega}_p$ is approximately equal to 1. For $\bar{\Omega}_p > 1$, the value of the group index decreases due to the power broadening of the transparency window. Meanwhile, the absorption coefficient decreases monotonically as $\bar{\Omega}_p$ increases. As a result, the characteristic spectral resolution $\delta\nu_c$ rapidly becomes smaller first as $\bar{\Omega}_p$ increases from zero, and $\delta\nu_c$ gradually approaches its theoretical limit $2\gamma_{ca}$ for $\bar{\Omega}_p > 2$ [see Fig. 6(c)]. On the other hand, one sees from Fig. 6(d) that the working finesse is approximately equal to the value of the normalized Rabi frequency $\bar{\Omega}_p$ as predicted in Eq. (46).

Note also that the characteristic resolution of an EIT medium is limited by the decay rate between the two ground states, which is typically much less than the linewidth of the transition between the excited state and one ground state. Therefore, a slow-light interferometer based on EIT can potentially achieve higher spectral resolution as compared to an interferometer based on double-absorption lines.

4. SUMMARY

In conclusion, the spectral performance of various types of slow-light interferometers has been studied under the practical situations in which the slow-light medium has associated gain or absorption and dispersion of the group index. We have shown that under practical conditions the actual spectral resolution of the interferometer is primarily limited by the ratio between the associated gain or loss and the group index, and that the working bandwidth is limited by the frequency dependence of this ratio.

The spectral performance of slow-light interferometers using three specific slow-light processes has been evaluated in terms of the characteristic spectral resolution and the working finesse. It has been shown that, while the characteristic resolution is typically limited by the linewidth of a resonance-induced slow-light medium, it can be much smaller if a broadband absorption or gain can be added on the narrow gain or absorption feature to make the slow-light medium more transparent over the spectral region for which the group index is large. Moreover, it has been shown that there is no fundamental upper limit for the working finesse that a slow-light interferometer can achieve. Of the three types of slow-light processes studied in this paper, EIT media have the potential to achieve the finest spectral resolution, because the linewidth is limited by the decay rate between two ground states, which is typically much less than that of a transition between an excited state and a ground state. However, double-absorption-line media have more applicability because it can be more easily implemented and controlled [17]. These analyses provide guidelines for how to choose appropriate slow-light techniques for interferometry applications to meet specific demands on the spectral performance.

ACKNOWLEDGMENTS

This work was supported by the Defense Advanced Research Projects Agency/Defense Sciences Office (DARPA/DSO) Slow Light program and by the National Science Foundation (NSF).

REFERENCES

1. R. W. Boyd and D. J. Gauthier, "'Slow' and 'fast' light," in *Progress in Optics*, Vol. 43, E. Wolf, ed. (Elsevier, 2002), pp. 497–530.
2. S. E. Harris and L. V. Hau, "Nonlinear optics at low light levels," Phys. Rev. Lett. **82**, 4611–4614 (1999).
3. M. S. Bigelow, N. N. Lepeshkin, and R. W. Boyd, "Observation of ultraslow light propagation in a ruby crystal at room temperature," Phys. Rev. Lett. **90**, 113903 (2003).
4. M. S. Bigelow, N. N. Lepeshkin, and R. W. Boyd, "Superluminal and slow light propagation in a room-temperature solid," Science **301**, 200–202 (2003).
5. G. M. Gehring, A. Schweinsberg, C. Barsi, N. Kostinski, and R. W. Boyd, "Observation of backwards pulse propagation through a medium with a negative group velocity," Science **312**, 895–897 (2006).
6. Y. Okawachi, M. S. Bigelow, J. E. Sharping, Z. Zhu, A. Schweinsberg, D. J. Gauthier, R. W. Boyd, and A. L. Gaeta, "Tunable all-optical delays via Brillouin slow light in an optical fiber," Phys. Rev. Lett. **94**, 153902 (2005).
7. M. Herráez, K. Y. Song, and L. Thévenaz, "Optically controlled slow and fast light in optical fibers using stimulated Brillouin scattering," Appl. Phys. Lett. **87**, 081113 (2005).
8. P. Ku, C. Chang-Hasnain, and S. Chuang, "Variable semiconductor all-optical buffer," Electron. Lett. **38**, 1581–1583 (2002).
9. A. Schweinsberg, N. N. Lepeshkin, M. S. Bigelow, R. W. Boyd, and S. Jarabo, "Observation of superluminal and slow light propagation in erbium-doped optical fiber," Europhys. Lett. **73**, 218–224 (2006).
10. R. M. Camacho, M. V. Pack, and J. C. Howell, "Slow light with large fractional delays by spectral hole-burning in rubidium vapor," Phys. Rev. A **74**, 033801 (2006).
11. R. M. Camacho, M. V. Pack, J. C. Howell, A. Schweinsberg, and R. W. Boyd, "Wide-bandwidth, tunable, multiple-pulse-width optical delays using slow light in cesium vapor," Phys. Rev. Lett. **98**, 153601 (2007).
12. R. W. Boyd, D. J. Gauthier, A. L. Gaeta, and A. E. Willner, "Maximum time delay achievable on propagation through a slow-light medium," Phys. Rev. A **71**, 023801 (2005).
13. R. W. Boyd and P. Narum, "Slow- and fast-light: fundamental limitations," J. Mod. Opt. **54**, 2403–2411 (2007).
14. S. M. Shahriar, G. Pati, V. Gopal, R. Tripathi, G. Cardoso, P. Pradhan, M. Messal, and R. Nair, "Precision rotation sensing and interferometry using slow light," in *Quantum Electronics and Laser Science Conference (QELS)*, (2005), paper JWB97.
15. Z. Shi, R. W. Boyd, D. J. Gauthier, and C. C. Dudley, "Enhancing the spectral sensitivity of interferometers using slow-light media," Opt. Lett. **32**, 915–917 (2007).
16. G. S. Pati, M. Salit, K. Salit, and M. S. Shahriar, "Demonstration of a tunable-bandwidth white-light interferometer using anomalous dispersion in atomic vapor," Phys. Rev. Lett. **99**, 133601 (2007).
17. Z. Shi, R. W. Boyd, R. M. Camacho, P. K. Vudyasetu, and J. C. Howell, "Slow-light Fourier transform interferometer," Phys. Rev. Lett. **99**, 240801 (2007).
18. C. Roychoudhuri, "Multiple-beam interferometers," in *Optical Shop Testing*, D. Malacara, ed. (Wiley, 1992), p. 213.
19. J. Sharping, Y. Okawachi, and A. Gaeta, "Wide bandwidth slow light using a Raman fiber amplifier," Opt. Express **13**, 6092–6098 (2005).
20. M. D. Stenner, M. A. Neifeld, Z. Zhu, A. M. Dawes, and D. J. Gauthier, "Distortion management in slow-light pulse delay," Opt. Express **13**, 9995–10002 (2005).

21. Z. Shi, R. Pant, Z. Zhu, M. D. Stenner, M. A. Neifeld, D. J. Gauthier, and R. W. Boyd, "Design of a tunable time-delay element using multiple gain lines for increased fractional delay with high data fidelity," Opt. Lett. **32**, 1986–1988 (2007).
22. M. D. Lukin, M. Fleischhauer, A. S. Zibrov, H. G. Robinson, V. L. Velichansky, L. Hollberg, and M. O. Scully, "Spectroscopy in dense coherent media: line narrowing and interference effects," Phys. Rev. Lett. **79**, 2959–2962 (1997).
23. M. Fleischhauer, A. Imamoglu, and J. P. Marangos, "Electromagnetically induced transparency: optics in coherent media," Rev. Mod. Phys. **77**, 633–673 (2005).